Journal of the Physical Society of Japan
Vol. 63, No. 1, January, 1994, pp. 66–77

Optical Stark Spectroscopy of a Brownian Oscillator in Intense Fields

Yoshitaka TANIMURA and Shaul MUKAMEL

Department of Chemistry, University of Rochester, Rochester, New York 14627

(Received July 22, 1993)

The optical Stark effect of a two-level system coupled to a Brownian oscillator (i.e. a harmonic mode which in turn is coupled to a heat bath) is studied using equations of motion for a reduced density matrix. These equations, derived using path integral techniques, can be used to study the combined effects of strong fields and dephasing processes at finite temperature, and interpolate continuously from the coherent to the overdamped limits where they reduce to the stochastic Gaussian-Markovian equation. Numerical calculations of probe absorption spectra for various pump intensities are presented, and show dynamical Stark splitting. In contrast to the Bloch equations which contain an infinite-temperature dephasing, we find that at finite temperature, the Stark peaks may have different heights even when the pump pulse is on resonance.

§1. Introduction

Femtosecond spectroscopy, such as impulsive Raman, optical Kerr, and pump-probe spectroscopy, provides a direct means for studying nuclear dynamics in the condensed phase.[1-6] Recent development of experimental techniques makes it possible to study high-order optical processes, induced by a sequence of pulses or a strong laser field.[7-9] It was predicted for example that a strong laser field can be used to localize an electron in one of the wells of a semiconductor double-well structure.[10] Intense field spectroscopy may provide useful information regarding dephasing processes; however, its theoretical analysis is much more complex compared with lower order processes.[11-15] The response function approach,[16] which is based on a perturbative expansion of the optical polarization in powers of the laser fields, has been successfully applied to study four-wave mixing experiments.[3,17] Calculation of the signal using the response function involves an N fold time integration for an N'th order optical process, and the number of the necessary terms (2^N Liouville space paths) rapidly grows with the order of the optical process. Thus, it is not easy to apply the response function to high-order optical processes.

Alternatively, optical processes can be calculated using a direct integration of the equations of motion in the presence of the fields. By calculating the relevant wave function[15] or density matrix elements,[18-22] it becomes possible to explore optical processes of arbitrary order. A difficulty with this approach is the proper treatment of dephasing processes induced by a heat bath. These are usually incorporated using equations of motion for a reduced density matrix, such as the optical Bloch equations. Effects of the bath are then taken into account by introducing a dephasing rate $1/T_2$, which can be obtained by assuming Gaussian-white noise fluctuations of the two-level frequency. The Bloch equations have the form

$$\frac{\partial}{\partial t}\hat{\rho}(t)=-i\mathscr{L}_{\rm eff}(t)\hat{\rho}(t), \tag{1}$$

where $\hat{\rho}(t)$ is the reduced density matrix of the two-level system, and $\mathscr{L}_{\rm eff}$ is the effective Liouville operator which includes relaxation terms (see eq. (30)). In many cases, the two level system is strongly coupled to nuclear degrees of freedom such as intramolecular vibrations, phonon modes, and solvent. The dynamics needs then to be described in the joint electronic and nuclear space, and it is not practical to treat all nuclear motions simply as a thermal bath. Once nuclear states are included explicitly in the density matrix, the number of

matrix elements grows rapidly. For p nuclear levels, the density matrix has p^2 elements and $\mathscr{L}_{\text{eff}}$ is a $p^2 \times p^2$ matrix. This makes the optical Bloch equations prohibitively hard to implement since it requires specifying and diagonalizing a large $\mathscr{L}_{\text{eff}}$ matrix. The problem becomes particularly severe in strong laser fields, where the number of relevant accessible nuclear states may become very large.

In this paper we consider a two-level system coupled to a harmonic mode which in turn is coupled to a heat bath.[3,17] This Brownian oscillator system may be described by the spin-Boson Hamiltonian with a proper choice of the spectral density.[23,24] Instead of dealing with phonon levels explicitly, we use path integral techniques to derive equations of motion for the reduced density matrix, which have a hierarchial form, and can be used to calculate the optical response of the system. This allows us to study the interplay of finite temperature dephasing and strong field effects over a broad range of parameters, whereby the oscillator changes from underdamped to overdamped. Using these equations of motion we predict the time and frequency dependent probe absorption following an excitation by an intense pump field.

§2. Probe Absorption Following a Strong Pump

Consider a pump-probe experiment, whereby the system is subjected to two light pulses: a strong pump and a weak probe, whose frequencies and wavevectors are denoted by Ω_1, $\boldsymbol{k}_1$ and Ω_2, $\boldsymbol{k}_2$, respectively. We assume that the laser frequencies Ω_1 and Ω_2 are close to the electronic transition frequency ω_{eg} of a two-level system. Then the Hamiltonian in the rotating wave approximation is:

$$H = H_A(t) + H_{\text{int}}, \tag{2}$$

where

$$H_A(t) = \frac{\hbar}{2}\omega_{eg}\sigma_z + \frac{\hbar}{2}\mu E_1(t)(e^{ik_1 r - i\Omega_1 t}\sigma_+ + e^{-ik_1 r + i\Omega_1 t}\sigma_-)$$
$$+ \frac{\hbar}{2}\mu E_2(t)(e^{ik_2 r - i\Omega_2 t}\sigma_+ + e^{-ik_2 r + i\Omega_2 t}\sigma_-), \tag{3}$$

$E_1(t)$ and $E_2(t)$ are the temporal envelopes of the pump and the probe fields, μ is the transition dipole matrix element, and σ_j represent the Pauli matrices defined by $\sigma_x \equiv |g\rangle\langle e| + |g\rangle\langle e|$, $\sigma_y \equiv i(|g\rangle\langle e| - |e\rangle\langle g|)$, $\sigma_z \equiv |e\rangle\langle e| - |g\rangle\langle g|$), and $\sigma_0 = 1$. We shall also use the combinations $\sigma_\pm \equiv (\sigma_x \pm i\sigma_y)/2$. The Hamiltonian H_{int} describes coupling of the two-level system to nuclear degrees of freedom. At this point, we need not specify H_{int} any further. Suffice is to say that the radiation field couples only to the electronic degrees of freedom (σ_j) and does not couple directly to the nuclear motions.

The probe absorption spectrum is commonly detected by spectrally dispersing the transmitted probe, and the signal is measured as a function of the dispersed frequency ω_2.[17] The dispersed spectrum is given by

$$S(\omega_2) = -2\,\text{Im}\,E_2[\omega_2]\,P_{k_2}[\omega_2], \tag{4}$$

where

$$E_2[\omega_2] = \frac{1}{\sqrt{2\pi}}\int_{-\infty}^{\infty} dt\,\exp(i\omega_2 t)E_2(t), \tag{5}$$

and

$$P_{k_2}[\omega_2] = \frac{1}{\sqrt{2\pi}}\int_{-\infty}^{\infty} dt\,\exp(i\omega_2 t)P_{k_2}(t). \tag{6}$$

The polarization $P(r, t)$ is defined by

$$P(r, t) \equiv \text{tr}\{\mu\sigma_x\hat{\rho}(t)\} = \sum_k e^{-ikr}P_k(t), \tag{7}$$

where $\hat{\rho}(t)$ is the total density matrix of the material system, and the trace is over all material degrees of freedom. We assume a weak probe and expand the polarization to first order in E_2. The polarization in the k_2 direction is then given by

$$P_{k_2}(t)=-\mathrm{i}\int_{-\infty}^{t}\mathrm{d}t'\,\mu E_2(t')\mathrm{e}^{-\mathrm{i}\Omega_2 t'}\,\mathrm{tr}\,\{[\sigma_-(t),\sigma_+(t')]\}. \tag{8}$$

Here, $\sigma_\pm(t)$ are the operators in the interaction picture

$$\sigma_\pm(t)\equiv\exp\left\{\frac{\mathrm{i}}{\hbar}\int_0^t\mathrm{d}\tau H_{\mathrm{A}}^0(\tau)\right\}\sigma_\pm\exp\left\{-\frac{\mathrm{i}}{\hbar}\int_0^t\mathrm{d}\tau H_{\mathrm{A}}^0(\tau)\right\}, \tag{9}$$

where

$$H_{\mathrm{A}}^0(t)\equiv\frac{\hbar}{2}\omega_{\mathrm{eg}}\sigma_z+\frac{\hbar}{2}\mu E_1(t)(\mathrm{e}^{-\mathrm{i}\Omega_1 t}\sigma_+ +\mathrm{e}^{\mathrm{i}\Omega_1 t}\sigma_-). \tag{10}$$

The present expression for the absorption spectrum (eq. (4) together with eq. (8)) is commonly used for strong continuous wave (cw) excitation.[11b,14]

It will be convenient in the following calculations to express the spectrum in the form of expectation values rather than a correlation function. This can be done as follows. Let us consider the evolution of the system subject only to the pump field. To that end we introduce the zero order Hamiltonian

$$H_0(t)\equiv H_{\mathrm{A}}^0(t)+H_{\mathrm{int}}, \tag{11}$$

and the corresponding solution of Liouville equation is denoted $\hat{\rho}^0(t)$:

$$\frac{\mathrm{d}}{\mathrm{d}t}\hat{\rho}^0(t)=-\frac{\mathrm{i}}{\hbar}[H_0(t),\hat{\rho}^0(t)]. \tag{12}$$

We next introduce a modified Hamiltonian which includes only the negative frequency component of E_2

$$H'(t)\equiv H_{\mathrm{A}}^0(t)+\hbar\mu E_2(t)\,\mathrm{e}^{-\mathrm{i}\Omega_2 t}\sigma_+ +H_{\mathrm{int}}. \tag{13}$$

The solution of the Liouville equation with this Hamiltonian will be denoted $\hat{\rho}'(t)$:

$$\frac{\mathrm{d}}{\mathrm{d}t}\hat{\rho}'(t)=-\frac{\mathrm{i}}{\hbar}[H'(t),\hat{\rho}'(t)]. \tag{14}$$

If we expand $\hat{\rho}'(t)$ to first order in the probe, we obtain

$$P_{k_2}(t)\approx 2\,\mathrm{tr}\,\{\sigma_-\langle\hat{\rho}'(t)-\hat{\rho}^0(t)\rangle\}=-\mathrm{i}\int_{-\infty}^{t}\mathrm{d}t'\,\mu E_2(t')\,\mathrm{e}^{-\mathrm{i}\Omega_2 t'}\,\mathrm{tr}\,\{[\sigma_-(t),\sigma_+(t')]\}$$
$$+\cdots. \tag{15}$$

The probe absorption spectrum (eq. (8)) can then be recast in the form

$$S(\omega_2)=-\sqrt{\frac{8}{\pi}}\,\mathrm{Im}\left\{E_2[\omega_2]\int_{-\infty}^{\infty}\mathrm{d}t\,\mathrm{e}^{\mathrm{i}\omega_2 t}\,\mathrm{tr}\,[\sigma_-\langle\hat{\rho}'(t)-\hat{\rho}^0(t)\rangle]\right\}. \tag{16}$$

We can thus calculate the absorption spectrum of a weak probe by subtracting two solutions of the Liouville equation! Equation (16) is the formal basis for the present calculations.

§3. Equations of Motion for the Reduced Density Matrix

We shall now consider a single Brownian oscillator coupled to our electronic two-level system. The interaction nuclear hamiltonian is assumed to be[25]

$$H_{\rm int}(\sigma_k, Q, x_j)=\frac{P^2}{2M}+\frac{1}{2}M\omega_0^2\left(Q+\frac{D}{2}\sigma_z\right)^2+\sum_j\left\{\frac{p_j^2}{2m_j}+\frac{1}{2}m_j\omega_j^2\left(x_j-\frac{c_j}{m_j\omega_j^2}Q\right)^2\right\}. \quad (17)$$

This model includes a single harmonic mode with Q, P, M, and ω_0 being its coordinate, momentum, mass, and frequency. The parameter D is the equilibrium displacement of the energy surfaces between the ground and the excited states (see Fig. 1). This mode is in turn coupled to a bath of harmonic oscillators with x_j, p_j, m_j, and ω_j denote their coordinates, momenta, masses, and frequencies. The constant c_j is the coupling strength to mode j. We use standard notation for the heat bath parameters. This mode coupled to a heat bath represents a Brownian oscillator.

Using a canonical transformation, the model Hamiltonian eq. (17) can be transformed into the spin-Boson Hamiltonian[23,24]

$$H_{\rm int}=\frac{1}{2}\sigma_z\sum_j c_j' x_j'+\sum_j\left(\frac{p_j'^2}{2m_j'}+\frac{1}{2}m_j'\omega_j'^2x_j'^2\right), \quad (18)$$

with the spectral density

$$J(\omega)\equiv\hbar\sum_j\left(\frac{c_j'^2}{4m_j'\omega_j'}\right)\delta(\omega-\omega_j')=\frac{\hbar^2\lambda}{\pi}\cdot\frac{\gamma(\omega)\omega_0^2\omega}{(\omega_0^2-\omega^2)^2+\gamma^2(\omega)\omega^2}, \quad (19)$$

where λ is a Stokes shift parameter

$$\lambda\equiv\frac{MD^2\omega_0^2}{2\hbar}, \quad (20)$$

and $\gamma(\omega)$ is a friction parameter

$$\gamma(\omega)\equiv\hbar\sum_j\left(\frac{c_j^2}{4m_j\omega_j^2}\right)\delta(\omega-\omega_j). \quad (21)$$

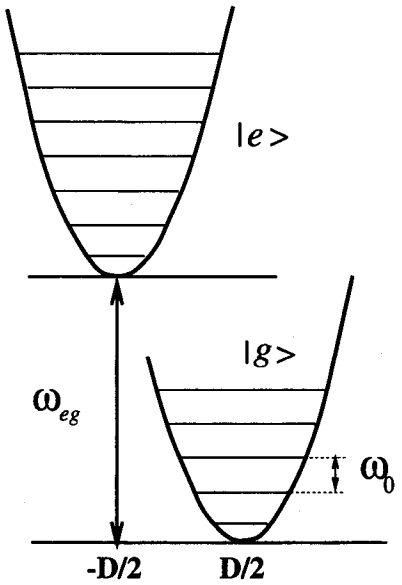

Fig. 1. Potential surfaces of the linearly displaced Brownian oscillator system. The lower electronic state is denoted $|g\rangle$, and the upper state is $|e\rangle$. The equilibrium coordinate displacement and electronic energy gap between the two potential are denoted by D and $\hbar\omega_{eg}$, respectively.

We shall be interested in calculating the reduced density matrix (traced over all nuclear coordinates). It has been shown that for any spectral density $J(\omega)$, one can derive equations of motion for the reduced density matrix of the two-level system in a hierarchial form.[26] In appendix A, we use path integral techniques to derive the reduced equations of motion for the present model using the spectral density (eq. (19)) with a frequency independent friction $\gamma(\omega)=\gamma$. The spectral density then has two poles $\gamma/2\pm i\zeta$, where $\zeta\equiv\sqrt{\omega_0^2-\gamma^2/4}$. The equations simplify considerably if the temperature of the heat bath is sufficiently high. We can then approximate $\coth(\beta\hbar\zeta/2)$ factors in the influence functional by $2/\beta\hbar\zeta$, where $\beta=1/K_BT$.[26] We have tested the range of validity of this approximation numerically for a weak pump excitation case, where an analytical expression of spectrum is known from the response function approach.[3] We found that the approximation holds provided $\beta\hbar\zeta\leq 4$. Under this condition the equations of motion can be expressed by a two dimensional hierarchy ρ_{nm}. We first introduce the reduced two-level density matrix traced over all nuclear degrees of freedom

$$\hat{\rho}_{00}(t)\equiv{\rm tr}_{Q,x_j}\{\hat{\rho}(t)\}. \quad (22)$$

The density matrix $\hat{\rho}_{00}(t)$ is then coupled to higher members of the hierarchy $\hat{\rho}_{nm}(t)$, defined in Appendix A. The equations of motion for $\hat{\rho}_{nm}(t)$ are

$$\frac{\partial}{\partial t}\hat{\rho}_{nm}(t)=-\left[\mathrm{i}\mathscr{L}_{\mathrm{A}}(t)+\frac{(n+m)\gamma}{2}+\mathrm{i}(m-n)\zeta\right]\hat{\rho}_{nm}(t)-\mathrm{i}\lambda\sigma_z^{\times}\left[\hat{\rho}_{n+1m}(t)+\hat{\rho}_{nm+1}(t)\right]$$
$$-n\mathrm{i}\Theta_-\hat{\rho}_{n-1m}(t)-m\mathrm{i}\Theta_+\hat{\rho}_{nm-1}(t),\quad (n,m\geq 0) \tag{23}$$

where

$$-\mathrm{i}\mathscr{L}_{\mathrm{A}}(t)\hat{\rho}(t)\equiv-\frac{\mathrm{i}}{\hbar}\{H_{\mathrm{A}}(t)\hat{\rho}(t)-\hat{\rho}(t)H_{\mathrm{A}}(t)\}=-\frac{\mathrm{i}}{\hbar}H_{\mathrm{A}}^{\times}(t)\hat{\rho}(t), \tag{24}$$

$$\Theta_{\pm}\hat{\rho}(t)\equiv\frac{1}{4}\left(\frac{2\zeta\pm\mathrm{i}\gamma}{2\beta\hbar\zeta}\sigma_z^{\times}\pm\frac{\omega_0^2}{2\zeta}\sigma_z^{\circ}\right)\hat{\rho}(t). \tag{25}$$

Here,

$$A^{\times}B=AB-BA,\quad A^{\circ}B=AB+BA, \tag{26}$$

for any ordinary operators A and B. The present equations take into account multiphonon absorption-emission processes. This infinite hierarchy can be truncated if carried out to a sufficiently high order $N\equiv n+m$ which satisfies $N\gg\Delta\Omega/\gamma$, where $\Delta\Omega$ is the Rabi frequency $\Delta\Omega\equiv\sqrt{(\Omega_1-\omega_{\mathrm{eg}})^2+(\mu E_1(t))^2}$. In Appendix B, we show that eq. (23) then becomes to[27]

$$\frac{\partial}{\partial t}\hat{\rho}_{N-mm}(t)=-\left[\mathrm{i}\mathscr{L}_{\mathrm{A}}(t)+\frac{N\gamma}{2}+\mathrm{i}(2m-N)\zeta\right]\hat{\rho}_{N-mm}(t)$$
$$-\lambda\sigma_z^{\times}\left[\frac{2(N-m+1)}{(N+1)\gamma+2\mathrm{i}(2m-N-1)\zeta}\Theta_-\right.$$
$$\left.+\frac{2(m+1)}{(N+1)\gamma+2\mathrm{i}(2m-N+1)\zeta}\Theta_+\right]\hat{\rho}_{N-mm}(t)$$
$$-\frac{2m\lambda}{(N+1)\gamma+2\mathrm{i}(2m-N-1)\zeta}\sigma_z^{\times}\Theta_+\hat{\rho}_{N-m+1m-1}(t)$$
$$-\frac{2(N-m)\lambda}{(N+1)\gamma+2\mathrm{i}(2m-N+1)\zeta}\sigma_z^{\times}\Theta_-\hat{\rho}_{N-m-1m+1}(t)$$
$$-\mathrm{i}(N-m)\Theta_-\hat{\rho}_{N-m+1m}(t)-im\Theta_+\hat{\rho}_{N-mm-1}(t).\quad (N\geq m\geq 0) \tag{27}$$

This N'th member of the hierarchy ($\hat{\rho}_{nm}(t)$ with $n+m=N$) is coupled only to lower members ($\hat{\rho}_{n'm'}(t)$ with $n'+m'\leq N$). The hierarchy can thus be terminated by choosing a sufficiently large N and using eq. (27), rather than eq. (23) for the N'th member. Equations (23) and (27) are most suitable for numerical computations. They require the solution of a coupled set of equation for $\hat{\rho}_{nm}(t)$ with $n+m\leq N$.

Let us consider now a few limiting cases. If $\gamma\gg\omega_0$ (strongly overdamped oscillator) the equations reduce to the tridiagnal Gaussian-Markovian hierarchy,[28]

$$\frac{\partial}{\partial t}\hat{\rho}_{n0}(t)=-[\mathrm{i}\mathscr{L}_{\mathrm{A}}(t)+n\gamma]\hat{\rho}_{n0}(t)-\mathrm{i}\lambda\sigma_z^{\times}\hat{\rho}_{n+10}(t)-n\mathrm{i}\Theta_-\hat{\rho}_{n-10}(t),\quad (n\geq 0) \tag{28}$$

and

$$\frac{\partial}{\partial t}\hat{\rho}_{N0}(t)=-[\mathrm{i}\mathscr{L}_{\mathrm{A}}(t)+N\gamma]\hat{\rho}_{N0}(t)-\frac{\lambda}{\gamma}\sigma_z^{\times}\Theta_-\hat{\rho}_{N0}(t)-N\mathrm{i}\Theta_-\hat{\rho}_{N-10}(t).$$
$$(N\gg\Delta\Omega/\gamma) \tag{29}$$

Note that in this limit $\hat{\rho}_{nm}(t)$ $(m>0)$ are decoupled from the hierarchy. The above equation is the quantum master equation for a Gaussian-Markovian bath, and is equivalent to the stochastic Liouville equation.[29]

In the Gaussian-white noise limit, $\gamma \gg \Delta\Omega$, we may further set $N=0$ and the equations reduce to

$$\frac{\partial}{\partial t}\hat{\rho}_{00}(t) = -\mathrm{i}\mathscr{L}_{\mathrm{A}}(t)\hat{\rho}_{00}(t) - \frac{1}{T_2}\sigma_z^{\times}\sigma_z^{\times}\hat{\rho}_{00}(t). \tag{30}$$

This is the quantum master equation, which is equivalent to the optical Bloch equation (1). The parameter $1/T_2 \equiv \lambda k_{\mathrm{B}} T/\hbar\gamma$ is the pure dephasing rate.

Using eq. (16), and eqs. (23) and (27), we can calculate the pump-probe spectrum. In the present notation, the first members of hierarchy $\hat{\rho}_{00}(t)$ and $\hat{\rho}'_{00}(t)$ are equal to $\hat{\rho}^0(t)$ and $\hat{\rho}'(t)$ in eq. (16), respectively. The final expression of the absorption spectrum is then

$$S(\omega_2) = -\sqrt{\frac{8}{\pi}}\,\mathrm{Im}\left\{E_2[\omega_2]\int_{-\infty}^{\infty} \mathrm{d}t\, \mathrm{e}^{\mathrm{i}\omega_2 t}\,\mathrm{tr}_{\mathrm{e}}\{\sigma_-(\hat{\rho}'_{00}(t) - \hat{\rho}_{00}(t))\}\right\}, \tag{31}$$

where the trace is only over the electronic two-level system space, since the other degrees of freedom have already been traced over.

§4. Numerical Results

We have calculated the probe absorption and its variation with time delay between the pump and the probe, for various pump intensities. We assume that both pulses are Gaussian $E_1(t) = E_1 \exp[-(t/\tau_1)^2]$ and $E_2(t) = E_2 \exp\{-[(t-T)/\tau_2]^2\}$ with resonance central frequencies, i.e. $\Omega_1 = \Omega_2 = \omega_{\mathrm{eg}}$. The pulse durations were taken to be $\tau_1 = 700$ [fs] and $\tau_2 = 30$ [fs] and the time delay was varied between $T = -2$ [ps] to $T = 1.0$ [ps]. The dynamical Stark effect shows up when the pump and the probe overlap in time. We used a weak probe with Rabi frequency $\delta_2 \equiv \mu E_2 = 10$ [GHz] and two values of pump intensities: medium intensity $\delta_1 \equiv \mu E_1 = 30$ [THz] and strong intensity $\delta_1 = 50$ [THz]. Initially at time $t = -15$ [ps] the two-level system is taken to be in the ground state. The Brownian oscillator parameters are $\omega_0 = 500$ [cm^{-1}], $D=1$, and the temperature $T = 200$ [K]. We have used two values of the friction $\gamma = 1500$ [cm^{-1}] (overdamped motion), and $\gamma = 50$ [cm^{-1}] (coherent, underdamped motion). In all calculations we set the hierarchy level at $N=30$, which yields $N(N+1)/2 = 465$ equations of motion for 2×2 density matrices $\hat{\rho}_{nm}(t)$ We then numerically integrated these differential equations using the Runge-Kutta 4'th method with a time step $\Delta t = 0.2$ (fs).

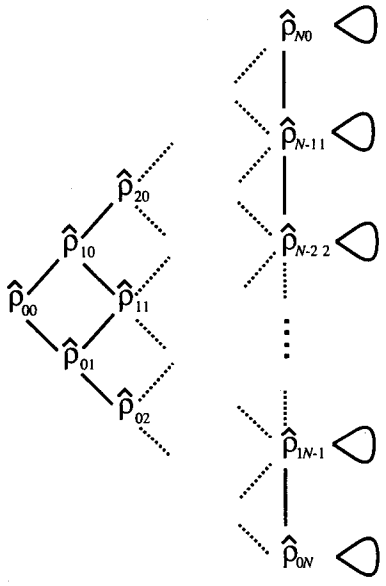

Fig. 2. Two-dimensional hierarchy of the density matrix equations. The matrices are connected by the equations of motion eq. (23), which are expressed by the lines in figure. Hierarchy level $(n+m)$ can be terminated by eq. (27) for $N \equiv (n+m) \gg \Delta\Omega/\gamma$, where $\Delta\Omega$ is the Rabi frequency of the system and γ is the relaxation constant of the heat bath. We then have a set of $N(N+1)/2$ equation of motion which involve the $N(N+1)/2$ 2×2 density matrices.

In Fig. 3(a), we show the results for the overdamped oscillator and the medium pump intensity $\delta_1 = 30$ [THz]. We set $\Delta\omega_2 \equiv \omega_2 - \omega_{\mathrm{eg}}$. The $T = -2$ [ps] curve corresponds to the linear absorption spectrum, since the pump is negligible at this early time. The overdamped oscillator does not show vibronic progressions

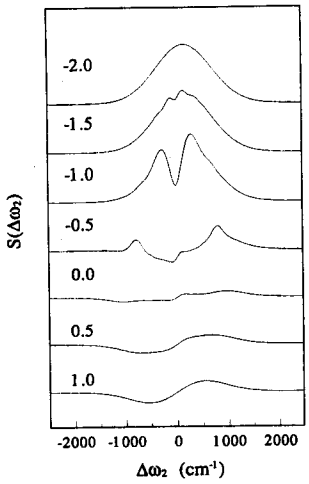

Fig. 3(a). Pump-probe spectrum for medium excitation strength ($\mu E_1=30$ [THz]) in the case of the overdamped oscillator for different pulse delays T (ps). For other parameters, see text.

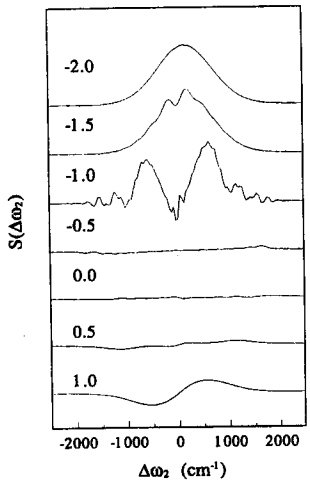

Fig. 4(a). Pump-probe spectrum for a strong excitation ($\mu E_1=50$ [THz]) in the case of the overdamped oscillator for different pulse delays T (ps). For other parameters, see text.

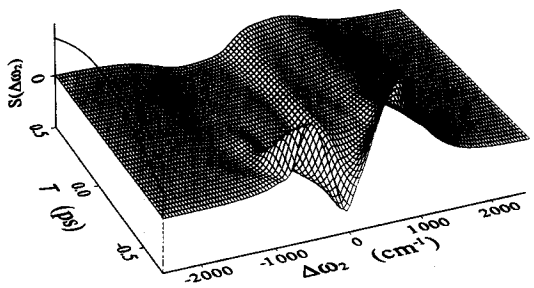

Fig. 3(b). Two-dimensional overview of Fig. 3(a). The trace above the T axis shows the pump envelope.

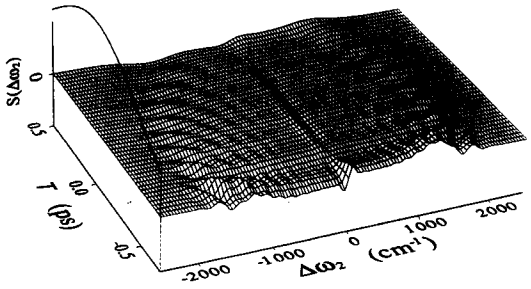

Fig. 4(b). Two-dimensional overview of Fig. 4(a). The trace above the T axis shows the pump envelope.

and the spectrum is Gaussian centered near $\Delta\omega_2=0$. The small 200 [cm^{-1}] shift to the blue reflects finite temperature effects.[30] This shift cannot be reproduced using the optical two-level Bloch equation[11] or the stochastic Liouville equation,[14] which neglect finite temperature effects on dephasing. As the delay is decreased, the Gaussian peak shows a dynamical Stark shift following the change of the pulse strength $\Delta\Omega_0=\sqrt{\Delta\omega_0^2+(\mu E_1(t))^2}$, where the detuning $\Delta\omega_0\equiv\Omega_1-\omega_{eg}=0$ for this resonant pump excitation. Figure 3(b) displays the same results in a two-dimensional plot which provides a global overview of the time dependent Stark shift. The blue Stark peak gives a positive contribution, whereas the red one becomes negative after $T=-0.5$ [ps]. In contrast, the Bloch equations or the stochastic Liouville equations predict both peaks to be identical. This again reflects the finite temperature of heat bath. Due to the Stark effect, the system has two Stark shifted excited states (dressed states). If the pump field is on resonance, and the temperature of the heat bath is infinite, then the populations of these two states are the same, as predicted by the Bloch or the stochastic Liouville equations. The population of the lower Stark level becomes higher than the upper Stark level. However, if the temperature of the bath is finite because of relaxation, then the upper level can absorb the probe field, whereas the lower level emits light, which gives a negative contribution to the probe absorption spectrum.

In Figs. 4(a) and 4(b), we show the probe absorption for the strong pump excitation

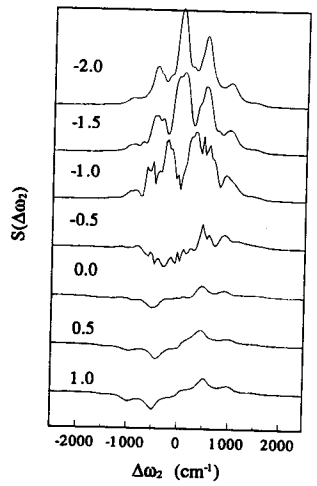

Fig. 5(a). Pump-probe spectrum for a medium pump strength ($\mu E_1 = 30$ [THz]) for an underdamped oscillator for different pulse, delays T (ps). For other parameters, see text.

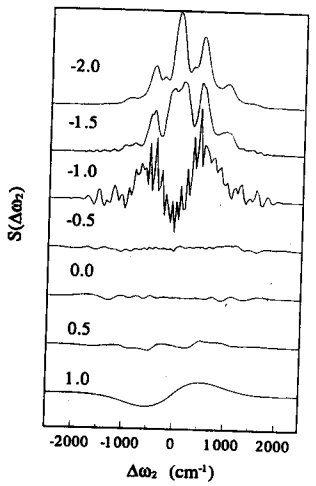

Fig. 6(a). Pump-probe spectrum for a strong excitation ($\mu E_1 = 50$ [THz]) for the underdamped oscillator for different pulse delays T (ps). For other parameters, see text.

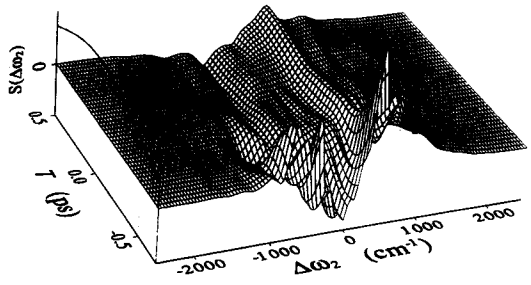

Fig. 5(b). Two-dimensional overview of Fig. 5(a). The trace above the T axis shows the pump envelope.

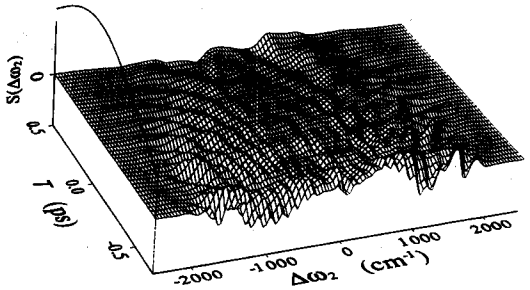

Fig. 6(b). Two-dimensional overview of Fig. 6(a). The trace above the T axis shows the pump envelope.

($\delta_1 = 50$ [THz]). Other parameters are the same as Figs. 3(a) and 3(b). For this strong excitation, the oscillator is pretty much decoupled from the system. We will discuss this point by comparing with the results for, the underdamped case (Figs. 6(a) and 6(b)).

Next we turn to the underdamped mode. Figures 5(a) and 5(b) show the pump-probe spectrum for medium pump strength. The $T = -2$ [ps] curve in Fig. 5(a) corresponds to the linear absorption spectrum. We have verified this by repeating these calculations using the response function approach. In this underdamped case, we observe the phonon side bands in the linear absorption spectrum at positions $\Delta\omega_2 = \pm n\omega_0$ corresponding to various phonon absorption-emission processes. Due to the finite temperature, the various phonon transitions yield an asymmetric lineshape. When the pump pulse is turned on, each phonon transition shows a Stark splitting whose magnitude is given by the proper Rabi frequency $\Delta\Omega_n = \sqrt{\Delta\omega_n^2 + (\mu E_1(t))^2}$; $\Delta\Omega_n$ is the Rabi frequency for the n'th vibrational line with $\Delta\omega_n = \pm n\omega_0$. In the early time periods the splitting of the peaks near the center are larger than for the side peaks (see curves for $T = -1.5$ [ps] and -1.0 [ps] in Fig 5(a)). This is because the corresponding Rabi frequency $\Delta\Omega_n$ changes significantly for small $\mu E_1(t)$ if $\Delta\omega_n$ is small. The Stark peaks of the origin ($\Delta\omega_0 = 0$) then shift to the blue and to the red. The positions of these peaks are the same as for the overdamped case, Fig. 3. The Stark shifted peaks of the phonon side bands can be observed outside of the Stark peaks of the

zero phonon line. Red Stark peaks show negative contributions, because of the finite temperature, as shown for the overdamped case.

Figures 6(a) and 6(b) display the pump-probe spectrum for the strong pump excitation. For this case, the results for the overdamped oscillator (Figs. 4(a) and 4(b)) and the present results for the underdamped oscillator are very similar. The oscillator seems to be decoupled from the optical transition and these spectra can be obtained using the two-level system alone. This can be explained using an argument first employed by Brewer;[12-14,31] under strong excitation, the relevant frequency of the atomic system is not ω_{eg} or ω_0, but rather Rabi frequency $\Delta\Omega_n \approx \mu E_1(t)$, which represents the "dressed" states.[32] For very strong excitation, this frequency is much larger than γ and ω_0. Thus the oscillator cannot respond to the system and the absorption spectrum approaches that of the isolated two-level system (without the brownian oscillator). This decoupling at strong fields can potentially be used to eliminate intramolecular vibrational relaxation and to enhance the selectivity of laser induced processes.[31]

§5. Concluding Remarks

We have analyzed the optical Stark effect of a two-level system coupled to a Brownian oscillator using equations of motion which allow us to incorporate finite temperature dephasing processes. The present approach can be applied to a system driven by pulses of arbitrary number, shape, and strength. It can be easily extended to multimode Brownian oscillator systems by introducing a higher dimensional hierarchy. For example, we can take into account two modes by introducing the equations of motion for the hierarchy matrix $\rho_{nm,kl}(t)$, where nm is the hierarchy for the first mode, and kl is the hierarchy for the second mode.

We may also apply this method to study charge transfer[33,34] or curve crossing[35-37] problems. The formal analogy between the calculation for optical processes in intense fields and the dynamics of nonadiabatic transitions such as curve crossing and charge transfer has been firmly established.[38] The analysis of optical processes as well as nonadiabatic transitions can be greatly enhanced by employing a less reduced density matrix in which the bath (x_j) modes are eliminated but we still keep the oscillator coordinates $\tilde{\rho}(t) \equiv \mathrm{tr}_x\{\rho(t)\}$. The density matrix $\tilde{\rho}(Q, P, t)$ can then be described as a wavepacket in phase space[3,17] by using the Wigner representation.[39] This should allow the development of a powerful semiclassical picture of nonadiabatic transitions. Phase space representations are well established for problems involving a single potential surface which have direct classical analog.[40,41] Their use in connection with electronic coherence was developed using the Langevin approach[17,34] and the extension to the present microscopic model should provide an additional insight.

Finally, the present approach can be used to study the Feynman polaron model, which is described by a particle interacting with a single phonon mode (LO phonon) with the frequency ω_{LO}.[42] If we introduce the Hamiltonian $H_A(t)$ defined in the coordinate space instead of the discrete two-level space, the hierarchy equations (23) with (27) then describe motions of a particle interacting with an oscillator mode.[27,43] If we set $\gamma \to 0$, then the oscillator mode becomes coherent and, thus, our model coincides with the Feynman polaron model ($\omega_{LO} = \omega_0$). This approach may be useful to study tunneling of Feynman polarons, where analytical solutions are not available.

Acknowledgements

The authors thank Dr. Michael Hartmann for useful discussions. The support of the NSF Center for Photoinduced Charge Transfer is gratefully acknowledged.

Appendix A: Derivation of the Hierarchy Equations Using Path Integrals

Consider the spin-Boson Hamiltonian

$$H(t) = H_A(t) + X(\sigma_i)\sum_j c_j x_j' + \sum_j \left(\frac{p_j'^2}{2m_j'} + \frac{1}{2} m_j' \omega_j'^2 x_j'^2 \right). \qquad (A\cdot 1)$$

The spectral distribution is given in eq. (19) with a frequency independent friction $\gamma(\omega)=\gamma$. $X(\sigma_j)$ is any function of $\sigma_j (j=x, y, z)$. The reduced density matrix of this system can be expressed in the path-integral form by using the coherent state representation, which is defined by the eigenfunctions of annihilation operator $\sigma_-|\phi\rangle=\phi|\phi\rangle$ and its conjugate $\langle\phi|\sigma_+=\langle\phi|\phi^*$, where ϕ is a Grassmann number.[28] The initial and the final states of the bra and ket are expressed by $\phi_i=\phi(t_i)$ and $\phi_i'^*=\phi'^*(t_i)$ and $\phi_f^*=\phi^*(t)$ and $\phi_f'=\phi'(t)$, respectively. If we denote a set of coherent state variable $\{\phi(t), \phi^*(t)\}$ by $\Phi(t)$, then the density matrix element at time t is given by[28a]

$$\rho(\Phi_f, \Phi_f'; t)=\int_{\Phi(t_i)=\Phi_i}^{\Phi(t)=\Phi_f} D[\Phi(t)] \int_{\Phi'(t_i)=\Phi_i'}^{\Phi'(t)=\Phi_f'} D[\Phi'(t)] \exp\left[\frac{i}{\hbar} S_A(\Phi; t, t_i)\right] \times F(\Phi, \Phi'; t, t_i) \exp\left[-\frac{i}{\hbar} S_A(\Phi'; t, t_i)\right], \quad (A\cdot 2)$$

where we have defined $\Phi_i=\{\phi_f, 0\}$, $\Phi_i'=\{0, \phi_i'^*\}$, $\Phi_f=\{0, \phi_f^*\}$, and $\Phi_f'=\{\phi_f', 0\}$. The functional $S_A(\Phi; t, t_i)$ is the action of H_A and $D[\Phi(t)]$ represents the functional integral of $\Phi(t)$. Since $J(\omega)$ has two poles $\gamma/2\pm i\zeta$, where $\zeta=\sqrt{\omega_0^2-\gamma^2/4}$, the influence functional $F(\Phi, \Phi'; t, t_i)$ is expressed as

$$F(\Phi, \Phi'; t, t_i)=\exp\left[(-i)^2 \int_{t_i}^{t} d\tau' \int_{t_i}^{\tau'} d\tau \{X(\Phi(\tau'))-X(\Phi'(\tau'))\} \times \{e^{-(\gamma/2+i\zeta)(\tau'-\tau)}\Theta_+(\Phi(\tau), \Phi'(\tau))+e^{-(\gamma/2-i\zeta)(\tau'-\tau)}\Theta_-(\Phi(\tau), \Phi'(\tau))\}\right], \quad (A\cdot 3)$$

where

$$\Theta_\pm(\Phi, \Phi')\equiv\frac{2\zeta\pm i\gamma}{2\beta\hbar\zeta}\{X(\Phi)-X(\Phi')\}\pm\frac{\omega_0^2}{2\zeta}\{X(\Phi)+X(\Phi')\}. \quad (A\cdot 4)$$

In the derivation of this expression we assumed that the initial temperature of the heat bath is high, ($\coth(\beta\hbar\zeta/2)\approx\beta\hbar\zeta/2$, where $\beta=1/K_BT$), and have employed the factorized initial condition

$$\hat{\rho}_{tot}(t_i)=\hat{\rho}(t_i)\hat{\rho}_B^e, \quad (A\cdot 5)$$

where $\hat{\rho}(t_i)$ is the initial density operator of the two-level system and $\hat{\rho}_B^e$ is the equilibrium density operator of the bath at inverse temperature β.

Consider the following elements:

$$\rho_{nm}(\Phi_f, \Phi_f'; t)\equiv\int_{\Phi(t_i)=\Phi_i}^{\Phi(t)=\Phi_f} D[\Phi(t)] \int_{\Phi'(t_i)=\Phi_i'}^{\Phi'(t)=\Phi_f'} D[\Phi'(t)] \left\{-ie^{-(\gamma/2-i\zeta)(t-\tau)}\int_{t_i}^{t} d\tau\Theta_-(\Phi(\tau), \Phi'(\tau))\right\}^n \times\left\{-ie^{-(\gamma/2+i\zeta)(t-\tau)}\int_{t_i}^{t} d\tau\Theta_+(\Phi(\tau), \Phi'(\tau))\right\}^m \times\exp\left[\frac{i}{\hbar} S_A(\Phi; t, t_i)\right] F(\Phi, \Phi'; t, t_i) \exp\left[-\frac{i}{\hbar} S_A(\Phi'; t, t_i)\right]. \quad (A\cdot 6)$$

Then $\rho_{00}(\Phi_f, \Phi_f'; t)$ agrees with $\rho(\Phi_f, \Phi_f'; t)$. The time differentiation of $\rho_{00}(\Phi_f, \Phi_f'; t)$ becomes

$$\frac{\partial}{\partial t}\rho_{00}(\Phi_f, \Phi_f'; t)=-i\mathcal{L}_A(\Phi_f, \Phi_f'; t)\rho_{00}(\Phi_f, \Phi_f'; t) -i\lambda\{X(\Phi_f)-X(\Phi_f)\}[\rho_{10}(\Phi_f, \Phi_f'; t)+\rho_{01}(\Phi_f, \Phi_f'; t)], \quad (A\cdot 7)$$

where

$$-i\mathscr{L}_A(\Phi_f, \Phi_f'; t) \equiv -\frac{i}{\hbar}\{H_A(\Phi_f; t) - H_A(\Phi_f'; t)\}. \tag{A·8}$$

The elements $\rho_{10}(\Phi_f, \Phi_f'; t)$ and $\rho_{01}(\Phi_f, \Phi_f'; t)$ can be evaluated by considering their time derivatives;

$$\begin{aligned}\frac{\partial}{\partial t}\rho_{10}(\Phi_f, \Phi_f'; t) = &-\left[i\mathscr{L}_A(\Phi_f, \Phi_f'; t) + \frac{\gamma}{2} - i\zeta\right]\rho_{10}(\Phi_f, \Phi_f'; t) \\ &-i\lambda\{X(\Phi_f) - X(\Phi_f)\}[\rho_{20}(\Phi_f, \Phi_f'; t) + \rho_{11}(\Phi_f, \Phi_f'; t)] \\ &-i\Theta_-(\Phi_f, \Phi_f')\rho_{00}(\Phi_f, \Phi_f'; t),\end{aligned} \tag{A·9}$$

and

$$\begin{aligned}\frac{\partial}{\partial t}\rho_{01}(\Phi_f, \Phi_f'; t) = &-\left[i\mathscr{L}_A(\Phi_f, \Phi_f'; t) + \frac{\gamma}{2} + i\zeta\right]\rho_{01}(\Phi_f, \Phi_f'; t) \\ &-i\lambda\{X(\Phi_f) - X(\Phi_f)\}[\rho_{11}(\Phi_f, \Phi_f'; t) + \rho_{02}(\Phi_f, \Phi_f'; t)] \\ &-i\Theta_+(\Theta_f, \Phi_f')\rho_{00}(\Phi_f, \Phi_f'; t).\end{aligned} \tag{A·10}$$

The above equation involve new elements $\rho_{nm}(Q_f, Q_f'; t)$, which can be evaluated by taking their time derivatives. For any n and m ($n, m \geq 0$), we have

$$\begin{aligned}\frac{\partial}{\partial t}\rho_{nm}(\Phi_f, \Phi_f'; t) = &-\left[i\mathscr{L}_A(\Phi_f, \Phi_f'; t) + \frac{(n+m)\gamma}{2} + i(m-n)\zeta\right]\rho_{nm}(\Phi_f, \Phi_f'; t) \\ &-i\lambda\{X(\Phi_f) - X(\Phi_f)\}[\rho_{n+1m}(\Phi_f, \Phi_f'; t) + \rho_{nm+1}(\Phi_f, \Phi_f'; t)] \\ &-ni\Theta_-(\Phi_f, \Phi_f')\rho_{n-1m}(\Phi_f, \Phi_f'; t) - mi\Theta_+(\Phi_f, \Phi_f')\rho_{nm-1}(\Phi_f, \Phi_f'; t).\end{aligned} \tag{A·11}$$

Equation (23) is the operator form of the above equation. Note that in the present description, we assumed the factorized initial condition eq. (A·5), which corresponds to $\rho_{00}(\Phi_i, \Phi_i'; t_i) = \rho(\Phi_i, \Phi_i'; t_i)$, and $\rho_{nm}(\Phi_i, \Phi_i'; t_i) = 0$. Correlated initial condition can be included by setting nonzero elements of $\rho_{nm}(\Phi_i, \Phi_i'; t_i)$.

Appendix B: Termination of the Hierarchy Equation

By using the Laplace transformation of eq. (23) and by assuming $N \gg \Delta\Omega/\gamma$, where $\Delta\Omega$ is the Rabi frequency $\Delta\Omega = \sqrt{(\omega_1 - \omega_{eg})^2 + (\mu E_1(t))^2}$, we have[27]

$$\hat{\rho}_{n+1m}(t) = -\frac{2i(n+1)}{(N+1)\gamma - 2i(n-m+1)\zeta}\Theta_+\hat{\rho}_{nm}(t) - \frac{2im}{(N+1)\gamma - 2i(n-m+1)\zeta}\Theta_-\hat{\rho}_{n+1m-1}(t), \tag{B·1}$$

and

$$\hat{\rho}_{nm+1}(t) = -\frac{2in}{(N+1)\gamma - 2i(n-m-1)\zeta}\Theta_+\hat{\rho}_{n-1m+1}(t) - \frac{2i(m+1)}{(N+1)\gamma - 2i(n-m-1)\zeta}\Theta_-\hat{\rho}_{nm}(t). \tag{B·2}$$

By inserting these equations into eq. (23), we obtain eq. (27).

References

1) P. C. Becker, R. L. Fork, C. H. Brito Cruz, J. P. Gordon and C. V. Shank: Phys. Rev. Lett. **60** (1988) 2462.
2) K. A. Nelson and E. P. Ippen: Adv. Chem. Phys. **75** (1989) 1.
3) S. Mukamel: Ann. Rev. Phys. Chem. 41 (1990) 647.
4) E. T. J. Nibbering, D. A. Wiersma and K. Duppen:

Phys. Rev. Lett. **66** (1991) 2464; E. T. J. Nibbering, K. Duppen and D. A. Wiersma: J. Chem. Phys. **93** (1990) 5477.
5) J. C. Lambry, J. Breton and J. L. Martin: Nature **363** (1993) 320.
6) G. R. Fleming: *Chemical Applications of Ultrafast Spectroscopy* (Oxford, New York, 1986).
7) N. F. Scherer, R. J. Carlson, A. Matio, M. Du, A. J. Ruggiero, V. Romero-Rochin, J. A. Cina, G. R. Fleming and S. A. Rice: J. Chem. Phys. **95** (1991) 1487.
8) S. D. Halle, M. Yoshizawa, H. Matsuda, S. Okada, H. Nakanishi and T. Kobayashi: submitted to Phys. Rev. Lett.
9) A. M. Weiner, D. E. Leaird, G. P. Wiederrecht and K. A. Nelson: Science **247** (1990) 1317.
10) F. Grossmann, T. Dittrich, P. Jung and P. Hänggi: Phys. Rev. Lett. **67** (1991) 516.
11) a) B. R. Mollow and M. M. Miller: Ann. Phys. **52**, 464 (1969); b) B. R. Mollow: Phys. Rev. **A5** (1972) 1523; c) B. R. Mollow: Phys. Rev. **A5** (1972) 2217; d) P. L. Knight and P. W. Milonni: Phys. Rep. **66** (1980) 21.
12) A. Schenzle, M. Mitsunaga, R. G. DeVoe, and R. G. Brewer: Phys. Rev. **A30** (1984) 325; R. G. DeVoe and R. G. Brewer: Phys. Rev. Lett. **50** (1983) 1269.
13) M. Yamanoi and J. H. Eberly: Phys. Rev. Lett. **52** (1984) 1453.
14) H. Tsunetsugu and E. Hanamura: J. Phys. Soc. Jpn. **55** (1986) 3636.
15) J. L. Krause, K. J. Schafer and K. C. Kulander: Phys. Rev. **A45** (1992) 4998.
16) N. Bloembergen: *Nonlinear Optics* (Benjamin, Massachusetts, 1965).
17) Y. J. Yan and S. Mukamel: J. Chem. Phys. **89** (1988) 5160; *ibid.* **94** (1991) 997; Y. J. Yan and S. Mukamel: Phys. Rev. **A41** (1990) 6485.
18) S. Schmitt-Rink and D. S. Chemla: Phys. Rev. Lett. **57** (1986) 2752; S. Schmitt-Rink, D. S. Chemla and H. Haug: Phys. Rev. **B37** (1988) 941.
19) R. Zimmermann and M. Hartmann: Phys. Status Solidi **B150** (1988) 365.
20) R. Binder, S. W. Koch, M. Lindberg, W. Schäfer and F. Jahnke: Phys. Rev. **B43** (1991) 6520.
21) H. Kühn, W. Vogel and D.-G. Welsch: J. Opt. Soc. Am. **B9** (1992) 1166.
22) B. W. Shore: *The Theory of Coherent Atomic Excitation* (John Wiley & Sons, New York, 1990) Vol. 1 and 2.
23) A. J. Leggett, S. Chakravarty, A. T. Dorsey, M. P. A. Fisher, A. Garg and Z. Zwerger: Rev. Mod. Phys. **59** (1987) 1.
24) A. Garg, J. N. Onuchic and V. Ambegaokar: J. Chem. Phys. **83** (1985) 4491.
25) Y. Tanimura and S. Mukamel: Phys. Rev. **E47** (1993) 118; Y. Tanimura and S. Mukamel: to be published in J. Opt. Soc. Am. **B**.
26) Y. Tanimura: Phys. Rev. **A41** (1990) 6676.
27) Y. Tanimura and P. G. Wolynes: Phys. Rev. **A43** (1991) 4137.
28) a) Y. Tanimura and R. Kubo: J. Phys. Soc. Jpn. **58** (1989) 101; b) *ibid*, **58** (1989) 1199; c) *ibid*, **58** (1989) 3001.
29) R. Kubo: in *Stochastic Processes in Chemical Physics*, ed. K. Shuler, (Wiley, New York, 1969) p. 101.
30) Y. Tanimura, T. Suzuki and R. Kubo: J. Phys. Soc. Jpn. **58** (1989) 1850.
31) S. Mukamel and K. Shan: Chem. Phys. Lett. **117** (1985) 489.
32) C. Cohen-Tannoudji and S. Haroche: J. Phys. (Paris) **30** (1969) 125; *ibid.* **30** (1969) 153.
33) G. C. Walker, E. Akesson, A. E. Johnson, N. E. Levinger and P. F. Barbara: J. Phys. Chem. **90** (1992) 3128; K. Tominaga, D. A. V. Kliner, A. E. Johnson, N. E. Levinger and P. Barbara: J. Chem. Phys. **98** (1993) 1228.
34) M. Sparpaglione and S. Mukamel: J. Chem. Phys. **88** (1988) 3263; *ibid.* **88** (1988) 4300.
35) J. Tully: J. Chem. Phys. **93** (1990) 1061.
36) F. Webster, P. J. Rossky and R. A. Friesner: Comput. Phys. Commun. **63** (1991) 494.
37) L. Khundkar and H. Zewail: Ann. Rev. of Phys. Chem. **41** (1990) 12.
38) S. Mukamel and Y. J. Yan: Acc. Chem. Res. **22** (1989) 301; Y. J. Yan and S. Mukamel: J. Phys. Chem. **93** (1989) 6991; Y. Hu and S. Mukamel: J. Chem. Phys. **91** (1989) 6973.
39) M. Hillery, R. F. O'Connel, M. O. Scully and E. P. Wigner: Phys. Rep. **106** (1984) 121.
40) W. H. Wells: Ann. Phys. **12** (1961) 1.
41) N. Hashitsume, M. Mori and T. Takahashi: J. Phys. Soc. Jpn. **55** (1986) 1887.
42) R. P. Feynman: Phys. Rev. **97** (1955) 660.
43) Y. Tanimura and P. G. Wolynes: J. Chem. Phys. **96** (1992) 8485.